A conserved epitope III on hepatitis C virus E2 protein has alternate conformations facilitating cell binding or virus neutralization

Lu Deng[a], Nancy Hernandez[a], Lilin Zhong[a], David D. Holcomb[a], Hailing Yan[a], Maria Luisa Virata[a], Sreya Tarafdar[a], Yanqun Xu[a], Yong He[a], Evi Struble[a], Harvey J. Alter[b,1], and Pei Zhang[a,1]

[a]Division of Plasma Protein Therapeutics, Office of Tissues and Advanced Therapies, Center for Biologics Evaluation and Research, Food and Drug Administration, Silver Spring, MD 20993-0002; and [b]Department of Transfusion Medicine, Warren Grant Magnuson Clinical Center, NIH, Bethesda, MD 20892

Contributed by Harvey J. Alter, May 28, 2021 (sent for review March 4, 2021; reviewed by Hubert E. Blum and Shan-Lu Liu)

Epitope III, a highly conserved amino acid motif of ^{524}APTYSW^{529} on the hepatitis C virus (HCV) E2 glycoprotein, resides in the critical loop that binds to the host receptor CD81, thus making it one of the most important antibody targets for blocking HCV infections. Here, we have determined the X-ray crystal structure of epitope III at a 2.0-Å resolution when it was captured by a site-specific neutralizing antibody, monoclonal antibody 1H8 (mAb1H8). The snapshot of this complex revealed that epitope III has a relatively rigid structure when confined in the binding grooves of mAb1H8, which confers the residue specificity at both ends of the epitope. Such a high shape complementarity is reminiscent of the "lock and key" mode of action, which is reinforced by the incompatibility of an antibody binding with an epitope bearing specific mutations. By subtly positioning the side chains on the three residues of Tyr^{527}, Ser^{528}, and Trp^{529} while preserving the spatial rigidity of the rest, epitope III in this cocrystal complex adopts a unique conformation that is different from previously described E2 structures. With further analyses of molecular docking and phage display–based peptide interactions, we recognized that it is the arrangements of two separate sets of residues within epitope III that create these discrete conformations for the epitope to interact selectively with either mAb1H8 or CD81. These observations thus raise the possibility that local epitope III conformational dynamics, in conjunction with sequence variations, may act as a regulatory mechanism to coordinate "mAb1H8-like" antibody-mediated immune defenses with CD81-initiated HCV infections.

HCV | epitope III | E2 protein | neutralization | conformation

Hepatitis C virus (HCV) infection is a major public health problem with ~71 million people worldwide who are chronically infected. A significant number of these patients will develop cirrhosis or liver cancer (1). While the advent of direct-acting antiviral agents has dramatically changed HCV treatment with high cure rates in the majority of patients (2–4), the development of a safe and effective HCV vaccine remains an unmet need for the global control of HCV infection.

Among other critical attributes, a successful vaccine counts on its capacity to elicit antibodies that can effectively neutralize the virus. In the case of HCV, an antibody with a broadly neutralizing capacity is rarely detectable, especially at the early stages of HCV infection (5), and if it is detectable at all, the antibody has yet to demonstrate its effectiveness in vivo. As a result, patients become chronically infected even in the presence of appreciable amounts of neutralizing antibodies (6). The underlying mechanism of how HCV manages to escape from antibody neutralization remains a major research challenge.

The E2 protein has long been regarded as the prime antibody target in efforts to generate a protective immunity (7–10). This importance of this viral envelope glycoprotein has been corroborated by studies demonstrating the essential role of the E2 protein in facilitating viral entry into hepatocytes via interactions with various host cell entry factors, chief among them CD81 (11–15).

The CD81-binding loop on the E2 protein is a segmental structure mapped to the amino acid residues between 523 and 540, of which Trp^{529} and, to a certain extent, Tyr^{527} are recognized as the most important residues for interacting with CD81 (16–18). As expected, most neutralizing antibodies target the CD81-binding loop (16, 18). Additionally, many other individual residues have also been implicated in CD81 interactions. Among them, several residues scattered in the region encompassing epitopes I and II, such as Trp^{420} and ^{436}GWLAGLFY^{443}, are of great relevance (17, 19–22).

To gain molecular insights into the E2–CD81 interface, we developed a monoclonal antibody, mAb1H8, that could block CD81-mediated entry of HCV by binding to a highly conserved amino acid motif inside the CD81-binding loop, known as epitope III (^{524}APTYSW^{529}) (18). By performing a series of mutational studies, we identified that the residues in this epitope could play a dual role by interacting with either mAb1H8 or CD81 through two distinct sets of its residues. The first set consisted of Ala^{524}, Pro^{525}, Tyr^{527}, Ser^{528}, and Trp^{529} for mAb1H8, while the second set consisted of Thr^{526}, Tyr^{527}, and Trp^{529} for CD81. Of note, both Ala^{524} and Pro^{525} were related only to the recognition by the antibody but not by CD81, a condition that could have an implication for viral escape from antibody responses. We thus proposed that there are two sets of residues in epitope III that can be spatially

Significance

Epitope III, a segment on the E2 glycoprotein of the hepatitis C virus (HCV) which binds to the host receptor CD81, is a key target for antibodies to block HCV entry. By solving the atomic structure of epitope III bound to a site-specific neutralizing antibody, mAb1H8, we showed that the epitope can adopt two distinct conformations by moving the side chains of its amino acids, allowing it to bind with either mAb1H8 or CD81. The coexistence of different conformational states of epitope III suggests its possible role in the regulation of antibody responses. These findings should help to design strategies to control HCV infection by tipping the balance toward epitope III conformations that favor antibody recognition rather than CD81 binding.

Author contributions: P.Z. designed research; L.D., N.H., L.Z., D.D.H., H.Y., M.L.V., S.T., Y.X., and Y.H. performed research; L.D., N.H., D.D.H., E.S., and H.J.A. contributed new reagents/analytic tools; L.D., N.H., D.D.H., M.L.V., and H.J.A. analyzed data; and L.D., M.L.V., H.J.A., and P.Z. wrote the paper.

Reviewers: H.E.B., University Hospital Freiburg; and S.-L.L., The Ohio State University.

The authors declare no competing interest.

[1]To whom correspondence may be addressed. Email: halter@dtm.cc.nih.gov or pei.zhang@fda.hhs.gov.

Published July 6, 2021.

arranged such that they are presented in two unique structured forms capable of functional duality (18).

Through a combinatorial approach that includes analyses by X-ray crystallography, computation, and biochemistry, we provide a line of evidence to suggest that it is the side-chain movements occurring on a few conserved residues that determine the coexistence of two epitope III conformational states, thereby allowing the same epitope to interact with either mAb1H8 or CD81.

Results

Overview of the Epitope III–mAb1H8 Complex Structure. Our postulation that the epitope III residues form different interfaces for engaging its partners during HCV infections prompted us to determine the crystal structure of epitope III. To minimize the possibility of inducible binding of the epitope peptides, we used an epitope III site-specific antibody, mAb1H8, to capture the conformation of the epitope. We chose mAb1H8 because it was generated after intentionally immunizing mice with a nearly full-length version of the E2 protein of the HCV H77 strain. Its neutralizing activity was then demonstrated in an in vitro cell-based infection assay (18).

To embody the functional characteristics of epitope III, a 15-mer peptide (^{520}DRSGAPTYSWGANDK^{534}) based on the HCV genotype 1 E2 protein sequence was chemically synthesized to contain most of the amino acids of the CD81-binding loop, wherein epitope III (APTYSW) was precisely mapped. The synthesized peptide was mixed with the Fab of mAb1H8 for the crystallization of the complex.

As shown in Fig. 1, all the complementarity-determining regions (CDRs) of the antibody were well-defined in the complex structure. The electron density of the peptide was clearly observed in the binding groove of the Fab region. Eight residues in the epitope III peptide between positions 523 and 530 were modeled into the electron-density map without ambiguity. However, the three N-terminal residues between positions 520 and 522 and the four C-terminal residues between positions 531 and 534 were not visible in the complex, suggesting that these seven residues did not form a stable structure and were dispensable for the antibody binding.

Description of the Epitope III–mAb1H8 Interface. Our previous analysis indicated that the epitope III residues Ala^{524}, Pro^{525}, Tyr^{527}, and Trp^{529} were among the most critical residues in the E2 protein for binding by mAb1H8 (18). In this epitope III–mAb1H8 structure, each of these epitope residues was found to be deeply buried in the complex (Fig. 1*A*). Noticeably, the residue Ala^{524}, along with its neighbor, Gly^{523}, was involved in contacting the residues in CDR3 of the heavy chain and CDR2 of the light chain, and encircled by the bulky side chains of Arg^{51} and Tyr^{54} of the light chain, where the methyl group on the alanine was confined within a cavity by van der Waals forces (Fig. 1*B*). The tightness between the epitope and the antibody at the site of Ala^{524} suggested that any replacement of Ala^{524} by an amino acid with a larger side chain, such as valine, would lead to a steric clash with the antibody (Fig. 1*C*). This structural feature correlated well with the fact that the mutation of Ala^{524} by a valine significantly reduced the binding of mAb1H8 to the E2 protein (18). As noted in our previous survey of the frequency at which an alanine is located at position 524 of the E2 protein, Val^{524} exists in ∼48% of all the HCV E2 protein sequences deposited in the National Institute of Allergy and Infectious Diseases Virus Pathogen Database and Analysis Resource (https://www.viprbrc.org/brc/home.spg?decorator=vipr) (18). The sequences with Val^{524} could thus represent the natural variants with a potential to escape in the presence of epitope III–specific antibodies, while maintaining their infectivity.

Of the four C-terminal residues in epitope III, the pair of Tyr^{527} and Trp^{529} has been linked to the folded structure of the E2 protein (18, 23–25). Mutation of either one of them could reduce the interaction between the E2 protein and CD81, although some of the reported conformational antibodies have reacted differently to these mutations (24). In the context of mAb1H8, both residues made multiple contacts with the CDR loops by forming a hydrogen-bond network between their side chains and the acidic residues Asp^{35} and Glu^{50} on the heavy chain (Fig. 1*A*). The tight interactions, along with the high shape complementarity, between these two aromatic bulky residues and mAb1H8 make any substitutions less tolerable, thus supporting a "lock and key" mode of action. By contrast, Ser^{528}, which appeared in 27% of natural variants of epitope III and is frequently replaced by Thr (20%) or Asn (43%) (18), interacted predominantly with the CDR loops of the light chain (Fig. 1*A*).

Epitope residue Pro^{525} was found to contact loosely with CDR1 and CDR2 on the light chain of the antibody (Fig. 1*A*). This structural feature is somewhat contrary to the observed fragility of antibody response to the presumed shape changes in recognizing the epitope with a Pro^{525}>Ala mutation (18). However, since Pro^{525} is extremely conserved among all HCV strains, a Pro^{525}>Ala mutant could not represent one of the natural variants for the virus to escape from epitope III–specific antibodies. Interestingly, a Pro^{525}>Ala mutation did not affect the CD81–E2 interaction. The highly conserved Pro^{525} may simply function as a locus for upholding the rigid structure in the E2 protein. Similarly, Thr^{526}, another highly conserved epitope residue, was positioned in a relatively spacious binding pocket (Fig. 1*A*), which enabled the antibody to have a certain degree of freedom to accept different amino acids at this site. This result was consistent with the observation that the Thr^{526}>Ala mutation of epitope III had little, if any, effect on the mAb1H8 binding to the E2 protein, although it severely weakened the E2–CD81 interaction (18). These results suggest to us that mAb1H8 was capable of selecting epitope III in a relatively rigid form and, in turn, neutralized the virus by locking the epitope in a defined conformation.

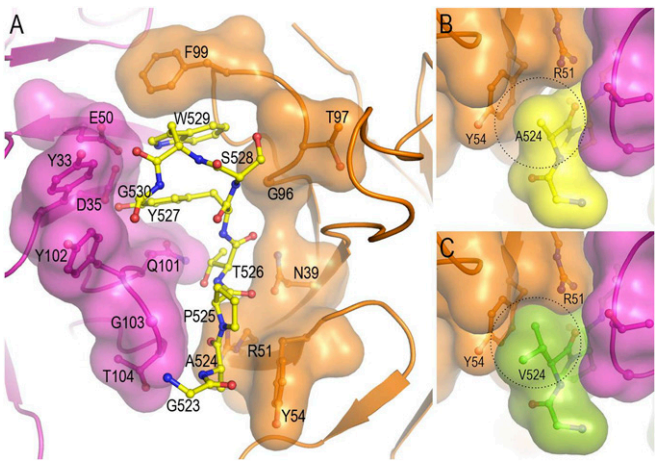

Fig. 1. Interactions between epitope III and mAb1H8. The antibody heavy chain is shown in magenta, the light chain in orange, and epitope III in yellow. (*A*) Key contacts between mAb1H8 and epitope III. (*B*) Surface representation of mAb1H8 and epitope III showing the tight fit between the side chains of Arg^{51} and Tyr^{54} of the mAb1H8 light chain and Ala^{524} of epitope III. (*C*) Potential steric clash between Val^{524} of the epitope III variant (in green) and Tyr^{54} of the mAb1H8 light chain.

An Alternate Conformation of Epitope III. We asked whether the conformation of epitope III varies while the epitope is free from binding by a site-specific antibody. To answer this question, we examined the epitope structures that were previously reported in the context of various forms of E2 complexed with a variety of antibodies (23, 26, 27). Since epitope III was located farther away from the reported antibody binding sites, we inferred that the

conformations of epitope III in these E2 structures represent unbound forms of the epitope.

Epitope III, when isolated from these E2 structures, showed a very similar shape. However, epitope III, when bound by mAb1H8, was found to be distinct (Fig. 2*A*). The rmsd was calculated in the range of 2.1 to 2.4 Å. The contours generated by the three N-terminal residues (Ala^{524}, Pro^{525}, and Thr^{526}) under both conditions were superimposable; however, the side chains of Tyr^{527}, Ser^{528}, and Trp^{529} at the C terminus in the presence of mAb1H8 projected toward different directions from those in the absence of mAb1H8, with respect to the axial reference assumed by the skein $^{524}APT^{526}$ (Fig. 2 *B* and *C*).

To further determine whether the conformation identified in this study represented a novel form of epitope III, Protein Data Bank (PDB) sequences were aligned against the sequence of the E2 ectodomain (23, 26, 27), and the atomic coordinates for the segment aligning with epitope III "APTYSWG" were extracted to generate an rmsd clustering heatmap by using the SVDSuperimposer package in the Biopython library. We found that epitope III in the complex with mAb1H8 had a unique conformation relative to all other E2 structures (Fig. 3*A*). Noticeably, epitope III was found to be clustered with both PDB ID codes 4WEB and 4WMF against all other E2 structures. Additionally, although epitope III was clustered with PDB ID codes 4WMF and 4WEB for structural similarity, it was clustered with the other E2 structures for sequence similarity. These observations allowed us to conclude that the structural uniqueness was not merely due to sequence differences (Fig. 3*B*).

Given the unique properties of epitope III, we asked whether mAb1H8 could recognize the epitope III conformations of the other E2 structures described in the PDB. Since all the known E2 structures appeared to adopt a similar scaffold, the E2 ectodomain complexed with a neutralizing antibody, HEPC74 (PDB ID code 6MEH), was chosen as a model for our further analysis (Fig. 4). When the epitope III–mAb1H8 complex structure was mounted onto the E2 structures by aligning the common epitope III sequence, all six CDR loops of mAb1H8 were found to interfere with multiple parts of E2 in the current E2 conformations, indicating that steric clashes would occur to prevent mAb1H8 from binding to E2. Therefore, E2 is likely to adopt an alternate conformation when it is bound by mAb1H8, implying that a conformational transition is required for E2 to be recognized by mAb1H8.

Epitope III Conformational State-Specific for CD81 Interaction. In light of the different roles of individual residues of epitope III in their selective engagement with mAb1H8 and CD81, we asked if epitope III, when it is not occupied by an antibody, as it was seen in the E2 core, could shift its residues into a specific conformation suitable for CD81 binding.

Previously, we showed that Tyr^{527} and Trp^{529} in epitope III are critical for CD81 binding and that Ala^{524}, Pro^{525}, and Ser^{528} are replaceable without disturbing the CD81 binding (18). Because Ser^{528} in epitope III is interchangeable with asparagine or threonine in the natural HCV variants, we tested Asn^{528}- and Thr^{528}-substituted peptides, assuming they take the same conformation displayed on the E2 structure, to see if they could dock onto the crystal structure of the human CD81 large extracellular domain (CD81-LEL) by using the Rosetta FastRelax protocols (Fig. 5). We found that all these peptides upheld the low-energy backbone and side-chain conformations with a nearly identical side-chain orientation that could dock equally onto a single motif on CD81-LEL, specifically the *d* helix. These results were in line with our finding that the E2 variant with a Ser^{528}>Ala substitution did not affect the CD81 binding (18).

To test whether the epitope III peptide could be physically associated with peptides containing the *d* helix of CD81-LEL, we performed random peptide phage display–screening experiments using the epitope III peptides as bait (Table 1). As Ala^{524} of epitope III was irrelevant to CD81 binding, it was purposely removed from the epitope peptides. In addition, because Ser^{528} was interchangeable with Asn^{528} in the natural variants without an impact on CD81 binding, two separate peptides, namely the S peptide (PTYSWGGSGGS) and the N peptide (PTYNWGGSGGS), containing Ser^{528} and Asn^{528}, respectively, were thus included in this experiment. We found several phage-displayed peptides that mimicked the "*d* helix" (i.e., $^{182}ISNLFKE^{188}$), particularly at the residue positions Ser^{183} and Asn^{184}. In addition, Lys^{187} and Glu^{188} of the *d* helix could be replaced by similar types of amino acids, arginine and aspartic acid, respectively, despite varying their linear positions in these "CD81-like" peptide mimics (Table 1). This result provided experimental evidence, as predicted by our computational simulation, that the epitope III peptide could present an alternate conformation suitable for CD81 interaction in the absence of a site-specific antibody, such as mAb1H8.

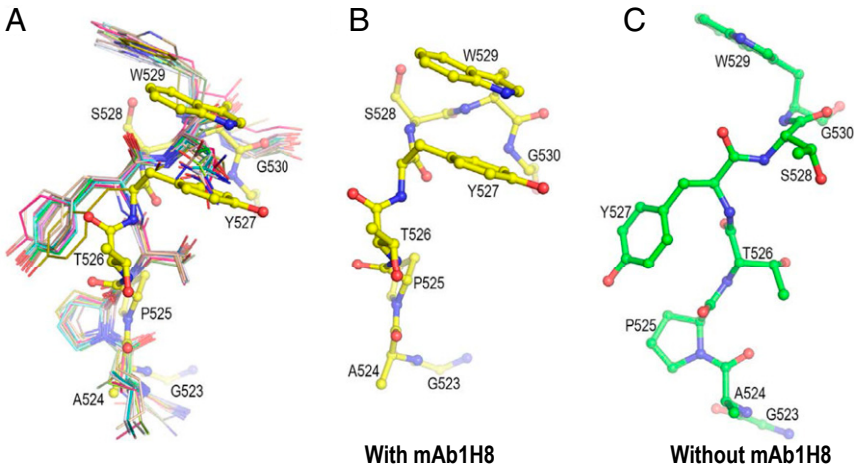

Fig. 2. Comparison of epitope III conformations from different complex structures. (*A*) Superimposition of epitope III currently available in the PDB onto the mAb1H8-bound form of epitope III. The PDB ID codes from which the coordinates of epitope III were extracted are 6URH, 6MEH, 6MEK, 6MEJ, 6MEI, 6WO3, 6WO5, 6WO4, 6WOQ, 6UYM, 6UYD, 6UYG, 6UYF, 4MWF, 6BKB, 6BKD, and 6BKC. (*A* and *B*) Side-chain projections of alternate epitope III conformations identified in the presence of mAb1H8 (*B*) or in the absence of mAb1H8 (*C*). Pro^{525} serves as a central point of the epitope, in conjunction with Ala^{524} and Thr^{526}, forming an axis of reference for the trajectories of the side chains of Tyr^{527}, Ser^{528}, and Trp^{529}.

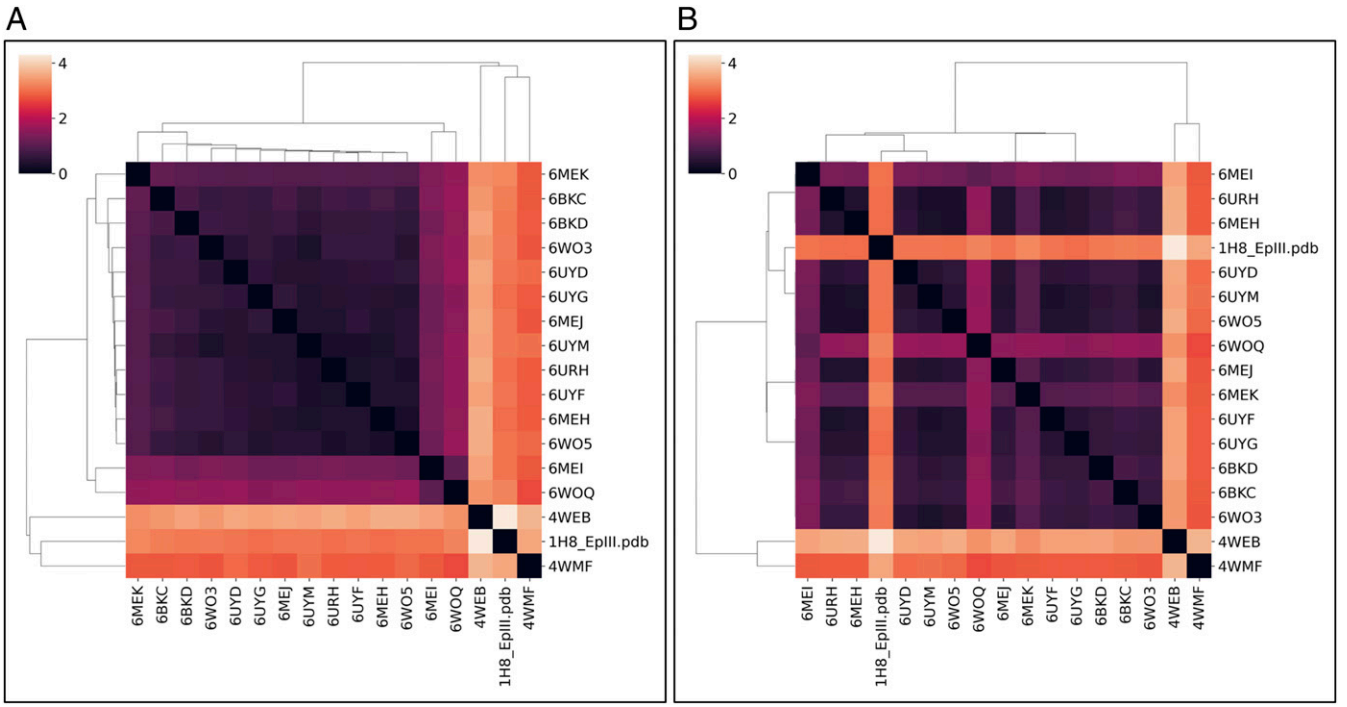

Fig. 3. Comparison of epitope III conformations with structures deposited in the PDB. (*A*) The hierarchical clustering heatmap derived from rmsd distances between epitope III conformations of crystal structures. Of these structures, PDB ID code 4WEB, epitope III, and PDB ID code 4WMF are outliers, as determined by the larger distance to other structures and by their classification into a cluster distant from the others. (*B*) The heatmap derived from distance measures in hierarchical clustering of epitope III sequences. While epitope III mapped in this study has a different amino acid sequence from others as depicted by the coloring in the heatmap, it is still clustered with the other structures contained in the PDB. As observed by the clustering, PDB ID codes 4WEB and 4WMF are different from others in terms of sequence.

Discussion

Protein is not a static object; instead, it is populated by a dynamic ensemble of various conformational states. The interconversions of these conformations, operating often in a variety of space and time scales, govern the different functions of the protein (28). In the case of HCV, the E2 protein is anticipated to be flexible, even though its core structure appears to be well-maintained by its intramolecular chemical bonds (26, 29–32). One of the consequences of such structural flexibility is the increased probability of the virus to prevent the host immune system from generating site-specific antibodies that can effectively neutralize the virus. In this study, we have presented a line of evidence to suggest that epitope III in the context of the E2 protein is no exception in this respect.

With mAb1H8, an antibody that binds specifically to epitope III and is able to neutralize the virus, we were able to capture the epitope in a conformational state that is different from those described previously regarding the CD81-binding loop of the HCV E2 structure. These conformational states of epitope III are linked with the subtle movements of the side chains in the C-terminal residues of the epitope, while the structural rigidity associated with the N-terminal residues is well-preserved. Consequently, the two resulting conformers exhibit distinct abilities in choosing their binding partners, either the antibody mAb1H8 or the host cell entry factor CD81.

The coexistence of two distinct forms of epitope III indicates a possibility of conformational equilibrium that may be established locally on the HCV E2 protein. If this is the case, the likelihood of each conformer occurring could be determined, in theory, by the relative free energies of these E2 conformers and, likewise, the rate of interconversion between them by the energy barrier of side-chain movements. However, the driving force for triggering this conformational transition remains to be investigated.

The conformational alternation as observed locally at epitope III cannot be viewed as an independent affair from other conformational deviations occurring at different regions on the E2 protein. More likely, each of these local conformational changes acts in accordance with maintaining a dynamic equilibrium globally at the level of the E2 protein. The different activities of the E2 protein are thus expected to correspond to discrete structures. For

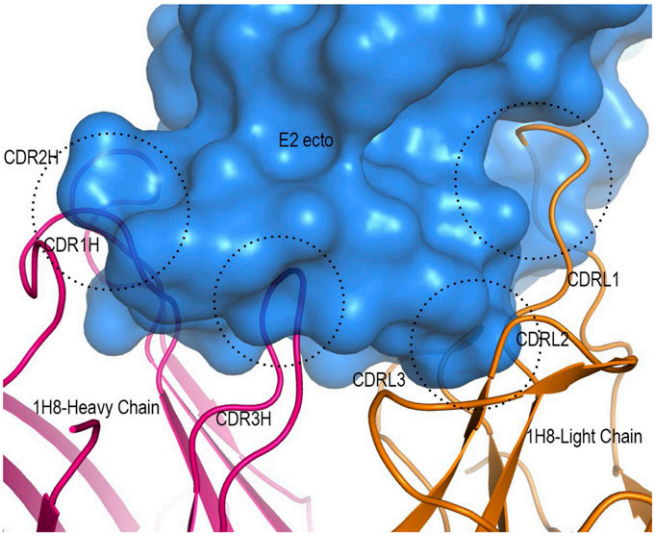

Fig. 4. Close-up view of the sites of steric clash between the CDR loops of mAb1H8 and E2 after superimposing epitope III bound with mAb1H8 onto that of the E2 ectodomain (PDB ID code 6MEH).

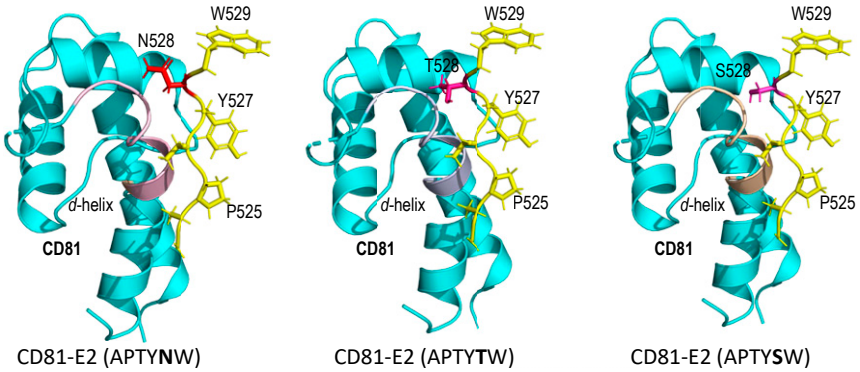

Fig. 5. Rosetta docking of the E2 structure with CD81. Three conformations of the epitope III peptide variants with the residues ^{525}PTYN (S, T) W^{529} restrained as observed in the E2 core structure are docked to the *d* helix of CD81-LEL (PDB ID code 5DFV). Residues of the epitope III peptide and CD81-LEL are shown in stick representation. Backbone and side-chain atoms of epitope III are indicated in yellow. The altered residues (Asn^{528}, Thr^{528}, and Ser^{528}) in the epitope are shown in red, magenta, and pink.

instance, the functionally related epitope II (^{437}WLAGLF^{442}) is hidden in the aforementioned E2 structures with some of its residues protruding into the cavity formed by the CD81-binding loop (21, 23). Despite epitope II being concealed, epitope II site-specific antibodies are still able to neutralize the virus, presumably by relying on the conformational changes occurring in E2 that can expose the epitope for antibody binding (20, 30, 33). To support this dynamic view, a recent study has uncovered the existence of an alternate conformer of E2 with its descriptive "neutralizing face" composed of the CD81-binding loop and the front layer of E2 (25).

According to the distributions of populated conformers, our findings may help to interpret the relationship between HCV infection and host immune defense. The dominance of conformers that are recognized by the epitope III residue-specific antibodies may skew antibody response toward virus neutralization. Conversely, the dominance of CD81-specific conformers could presumably increase the probability for the virus to enter liver cells, thus facilitating viral infections while avoiding antibody binding. Relevant to this interpretation, we previously showed that the antibodies with a specificity toward the epitope III residues could be produced in less than 15% of patients only when the chronic HCV infection had already been established (18). While this observation suggests an inadequate production of antibodies to epitope III during natural HCV infection, it raises the question of whether the conformational equilibrium plays a role in determining an antibody response in these patients.

It should be pointed out that a naturally occurring variant of epitope III, the Ala^{524}>Val substitution, where a larger side chain is introduced, is no longer structurally compatible with the binding pocket of mAb1H8. However, this epitope variant still retains its full capacity to bind CD81 (18). The appearance of Ala^{524} and Val^{524} variants reflects the selection pressure imposed by site-specific neutralizing antibodies that drives sequence evolution at epitope III during natural HCV infections, a general concept supported by several studies (34, 35). The highly conserved epitope III sequence not only stabilizes the epitope at specific positions, such as Tyr^{527} and Trp^{529}, for the structural rigidity needed for one function but also permits the subtle flexibility in the side chains, as seen in this case, for the other function.

These observations allow us to conclude that there are two independent mechanisms operating jointly at epitope III: The variation at specific positions, such as Ala^{524}>Val, offers a survival advantage for the virus under the selective pressure of the site-specific antibodies and, simultaneously, the high conservation of other epitope amino acids, such as Tyr^{527} and Trp^{529}, ensures the ability of the virus to preserve local conformational dynamics for ultimately modulating antibody responses and viral entry during infection. From uncovering these structural insights, our findings should help researchers design future experiments to test whether HCV infection could be controlled by tipping the balance of epitope III conformations to favor recognition by neutralizing antibodies.

Materials and Methods

Peptide Synthesis and Protein Preparation. All peptides were chemically synthesized by the Core Laboratory of the Center for Biologics Evaluation and Research at the US Food and Drug Administration, by using an Applied Biosystems model 433A peptide synthesizer as previously described (22, 33). Ascites containing mAb1H8 was produced by Harlan Bioproducts for Science as previously described (18). Fab of the immunoglobulin molecule was prepared using the Pierce Fab Preparation Kit (44985) from Thermo Fisher Scientific by following the instructions from the manufacturer.

Crystallization and Data Collection. Crystallization screenings were carried out robotically with a Mosquito liquid dispenser from SPT LabTech by the hanging-drop vapor-diffusion method (33). Crystals of the epitope III–mAb1H8 complex were grown in 20% polyethylene glycol 3350, 0.1 M citrate (pH 5.5) at 21 °C. Glycerol (20% volume/volume) was used as the cryoprotectant. X-ray diffraction data were collected at beamline X29 of the Brookhaven National Synchrotron Light Source with an ADSC Quantum-315 charge-coupled device detector. All data were indexed, integrated, and scaled with the program HKL2000 (36).

Structure Determination and Refinement. The structure of the epitope III–mAb1H8 complex was determined as previously described (33) by molecular replacement using Phaser (37) in CCP4 (38) with the anti-HCV epitope II antibody mAb#8 (PDB ID code 4HZL) as the search model (33). After refinement with RefMac 5.0 (39), the epitope III peptide was built into the resulting

Table 1. Identification of CD81-like peptides by screening random peptide phage display libraries

Epitope III peptide	Phage-displayed peptide	Residue similarity to those of CD81 (*d* helix I^{182}SNFKL^{188})
N peptide	ITNAPIKDLTP	I^{182}, S^{183}, N^{184}, F^{186}, K^{187}, E^{188}
	NSNDFRPGGPET	S^{183}, N^{184}, F^{186}, K^{187}
S peptide	SNKNLDTRILTK	S^{183}, N^{184}, F^{186}, E^{188}

N peptide: PTY**N**WGGSGGS-biotin; S peptide: PTY**S**WGGSGGS-biotin. Underline: amino acids identified that are similar or identical to the *d* helix.

difference electron-density map using the program Coot (40). The CDR loops were deleted in the initial refinement and built into where an unambiguous electron density was shown. There were two complexes in a crystallographic asymmetric unit with nearly identical conformations as indicated by the rmsd of 0.2 Å in the α-carbon atoms of the variable domain of the Fab molecules and the epitope III peptides. Contact residues in the epitope III–mAb1H8 complex were identified with the program Contact in CCP4 and were defined as residues containing an atom ≤4.0 Å from a residue of the binding partner. Buried surface areas were calculated by the program AreaIMol in CCP4 with a 1.4-Å probe radius. PyMOL (https://pymol.org/2/) was used to prepare the structural figures.

Rosetta Docking of the HCV E2 Structure with Human CD81. The crystal structure of HCV E2 protein (PDB ID code 4MWF) was used as a docking partner to human CD81 (PDB ID code 5DFV). The Rosetta Docking Protocol was implemented in ROSIE (Rosetta Online Server; https://rosie.graylab.jhu.edu/) to allow for the identification of possible binding sites (41–43). Manual inspection was then performed on the top-scoring structures.

Computational Analysis of Peptides with Rosetta FastRelax. The Rosetta FastRelax protocol (all-atom refinement) was performed on the docked structure to identify the low-energy backbone and side-chain conformations of the target peptides through 100 rounds of packing and minimization (fixed-backbone Rosetta energy minimization) (44, 45) and was also used to introduce mutations for comparisons. Comparison of the wild type (epitope III peptide) and variants (including the Ala^{524}>Val variant) was performed with the lowest scored energy-minimized structure.

Alignment of Epitope III Conformations Contained in the PDB. The E2 sequence was taken from PDB ID code 6MEH (26). This sequence was queried against the Protein Data Bank (46) using default values, and all matching structures were downloaded. For each matching structure, all chains were aligned with the PDB ID code 6MEH E2 sequence using Clustal Omega (47, 48). For the closest matching chain, atomic coordinates for the subsequence aligned to APTYSWG were extracted. When the subsequence did not exactly match APTYSWG, only matching atomic coordinates were taken. These coordinates were structurally aligned against our motif coordinates, and rmsd was calculated using the SVDSuperimposer package in the Biopython library (49). In addition, the rmsd's of motif coordinates for each pair of structures were compared. Finally, the rmsd's were used to compute a hierarchical clustering heatmap with the Seaborn Python library (50). To account for sequence differences between structures, we also computed the fraction of positions not matching between each pair of motifs, and used these values to create a hierarchical clustering heatmap.

Detection of the Interaction of Epitope III with CD81 by Phage Display. A random peptide phage-displayed library (Ph.D. 12-mer) was purchased from New England Biolabs. The peptides representing the wild-type epitope III and its variants were synthesized, respectively, with a biotin tag. These peptides were then utilized individually to screen the random peptides from the phage-displayed library using a precipitation procedure with streptavidin Dynabeads (Thermo Fisher Scientific) by following the protocols by the manufacturer. Briefly, ~10^{10} phages were incubated with biotinylated epitope peptide/streptavidin bead mixtures for 20 min at room temperature. After eight washings with 0.05 M Tris·HCl buffer (pH 7.5) containing 0.15 M NaCl and 0.05% Tween 20, the phages were eluted from the complex with 0.1 M HCl for 8 min at room temperature. The eluted phages were then amplified in the host strain ER2738. Amplified phages were subjected to three additional rounds of selection with the epitope peptide. After selection, collected phages were grown on Luria–Bertani broth (LB)-agar plates. DNA from each single-phage plaque was sequenced, and the corresponding peptide sequence was then deduced from the DNA sequence. The sequence homology of phage-displayed peptides with CD81-LEL was determined. The epitope-binding peptides with a high sequence homology to the CD81-LEL sequence were defined as CD81-like peptides.

Data Availability. The atomic coordinates and structure factors reported in this article have been deposited in the Protein Data Bank, https://www.wwpdb.org/ (PDB ID code 7LKI). All study data are included in the main text.

ACKNOWLEDGMENTS. We thank Howard Robinson at the Brookhaven National Synchrotron Light Source for X-ray data collection. Beamline X29 is supported by the US Department of Energy Offices of Biological and Environmental Research and Basic Energy Sciences and by the National Center for Research Resources of the NIH. This study used the computational resources of the High Performance Computing clusters at the Food and Drug Administration (FDA), Center for Devices and Radiological Health (CDRH). This study was funded by intramural research funds from the Center for Biologics Evaluation and Research (CBER), FDA. S.T. was supported by the Research Participation Program at the CBER, administered by the Oak Ridge Institute for Science and Education through an interagency agreement between the US Department of Energy and the FDA.

1. World Health Organization, Hepatitis C: Fact sheet (2021). https://www.who.int/news-room/fact-sheets/detail/hepatitis-c. Accessed 15 June 2021.
2. M. Götte, J. J. Feld, Direct-acting antiviral agents for hepatitis C: Structural and mechanistic insights. *Nat. Rev. Gastroenterol. Hepatol.* **13**, 338–351 (2016).
3. M. P. Manns *et al.*, Hepatitis C virus infection. *Nat. Rev. Dis. Primers* **3**, 17006 (2017).
4. M. Martinello, B. Hajarizadeh, J. Grebely, G. J. Dore, G. V. Matthews, Management of acute HCV infection in the era of direct-acting antiviral therapy. *Nat. Rev. Gastroenterol. Hepatol.* **15**, 412–424 (2018).
5. J. M. Pestka *et al.*, Rapid induction of virus-neutralizing antibodies and viral clearance in a single-source outbreak of hepatitis C. *Proc. Natl. Acad. Sci. U.S.A.* **104**, 6025–6030 (2007).
6. C. Logvinoff *et al.*, Neutralizing antibody response during acute and chronic hepatitis C virus infection. *Proc. Natl. Acad. Sci. U.S.A.* **101**, 10149–10154 (2004).
7. P. Farci *et al.*, Prevention of hepatitis C virus infection in chimpanzees by hyperimmune serum against the hypervariable region 1 of the envelope 2 protein. *Proc. Natl. Acad. Sci. U.S.A.* **93**, 15394–15399 (1996).
8. S. E. Frey *et al.*, Safety and immunogenicity of HCV E1E2 vaccine adjuvanted with MF59 administered to healthy adults. *Vaccine* **28**, 6367–6373 (2010).
9. J. L. Law *et al.*, A hepatitis C virus (HCV) vaccine comprising envelope glycoproteins gpE1/gpE2 derived from a single isolate elicits broad cross-genotype neutralizing antibodies in humans. *PLoS One* **8**, e59776 (2013).
10. M. Puig, M. E. Major, K. Mihalik, S. M. Feinstone, Immunization of chimpanzees with an envelope protein-based vaccine enhances specific humoral and cellular immune responses that delay hepatitis C virus infection. *Vaccine* **22**, 991–1000 (2004).
11. M. Flint *et al.*, Characterization of hepatitis C virus E2 glycoprotein interaction with a putative cellular receptor, CD81. *J. Virol.* **73**, 6235–6244 (1999).
12. K. Kitadokoro *et al.*, CD81 extracellular domain 3D structure: Insight into the tetraspanin superfamily structural motifs. *EMBO J.* **20**, 12–18 (2001).
13. G. Koutsoudakis, E. Herrmann, S. Kallis, R. Bartenschlager, T. Pietschmann, The level of CD81 cell surface expression is a key determinant for productive entry of hepatitis C virus into host cells. *J. Virol.* **81**, 588–598 (2007).
14. P. Pileri *et al.*, Binding of hepatitis C virus to CD81. *Science* **282**, 938–941 (1998).
15. J. Zhang *et al.*, CD81 is required for hepatitis C virus glycoprotein-mediated viral infection. *J. Virol.* **78**, 1448–1455 (2004).
16. L. Kong *et al.*, Structural flexibility at a major conserved antibody target on hepatitis C virus E2 antigen. *Proc. Natl. Acad. Sci. U.S.A.* **113**, 12768–12773 (2016).
17. A. M. Owsianka *et al.*, Identification of conserved residues in the E2 envelope glycoprotein of the hepatitis C virus that are critical for CD81 binding. *J. Virol.* **80**, 8695–8704 (2006).
18. Z. Zhao *et al.*, A neutralization epitope in the hepatitis C virus E2 glycoprotein interacts with host entry factor CD81. *PLoS One* **9**, e84346 (2014).
19. H. E. Drummer, I. Boo, A. L. Maerz, P. Poumbourios, A conserved Gly436-Trp-Leu-Ala-Gly-Leu-Phe-Tyr motif in hepatitis C virus glycoprotein E2 is a determinant of CD81 binding and viral entry. *J. Virol.* **80**, 7844–7853 (2006).
20. H. Duan *et al.*, Amino acid residue-specific neutralization and nonneutralization of hepatitis C virus by monoclonal antibodies to the E2 protein. *J. Virol.* **86**, 12686–12694 (2012).
21. C. Harman *et al.*, A view of the E2-CD81 interface at the binding site of a neutralizing antibody against hepatitis C virus. *J. Virol.* **89**, 492–501 (2015).
22. P. Zhang *et al.*, Hepatitis C virus epitope-specific neutralizing antibodies in Igs prepared from human plasma. *Proc. Natl. Acad. Sci. U.S.A.* **104**, 8449–8454 (2007).
23. L. Kong *et al.*, Hepatitis C virus E2 envelope glycoprotein core structure. *Science* **342**, 1090–1094 (2013).
24. R. Gopal *et al.*, Probing the antigenicity of hepatitis C virus envelope glycoprotein complex by high-throughput mutagenesis. *PLoS Pathog.* **13**, e1006735 (2017).
25. N. Tzarum *et al.*, An alternate conformation of HCV E2 neutralizing face as an additional vaccine target. *Sci. Adv.* **6**, eabb5642 (2020).
26. A. I. Flyak *et al.*, HCV broadly neutralizing antibodies use a CDRH3 disulfide motif to recognize an E2 glycoprotein site that can be targeted for vaccine design. *Cell Host Microbe* **24**, 703–716.e3 (2018).
27. A. I. Flyak *et al.*, An ultralong CDRH2 in HCV neutralizing antibody demonstrates structural plasticity of antibodies against E2 glycoprotein. *eLife* **9**, e53169 (2020).
28. K. Henzler-Wildman, D. Kern, Dynamic personalities of proteins. *Nature* **450**, 964–972 (2007).
29. A. G. Khan *et al.*, Structure of the core ectodomain of the hepatitis C virus envelope glycoprotein 2. *Nature* **509**, 381–384 (2014).
30. L. Deng *et al.*, Discrete conformations of epitope II on the hepatitis C virus E2 protein for antibody-mediated neutralization and nonneutralization. *Proc. Natl. Acad. Sci. U.S.A.* **111**, 10690–10695 (2014).
31. A. Meola *et al.*, Structural flexibility of a conserved antigenic region in hepatitis C virus glycoprotein E2 recognized by broadly neutralizing antibodies. *J. Virol.* **89**, 2170–2181 (2015).

32. A. D. Dearborn, J. Marcotrigiano, Hepatitis C virus structure: Defined by what it is not. *Cold Spring Harb. Perspect. Med.* **10**, a036822 (2020).
33. L. Deng *et al.*, Structural evidence for a bifurcated mode of action in the antibody-mediated neutralization of hepatitis C virus. *Proc. Natl. Acad. Sci. U.S.A.* **110**, 7418–7422 (2013).
34. K. A. Dowd, D. M. Netski, X. H. Wang, A. L. Cox, S. C. Ray, Selection pressure from neutralizing antibodies drives sequence evolution during acute infection with hepatitis C virus. *Gastroenterology* **136**, 2377–2386 (2009).
35. T. von Hahn *et al.*, Hepatitis C virus continuously escapes from neutralizing antibody and T-cell responses during chronic infection in vivo. *Gastroenterology* **132**, 667–678 (2007).
36. Z. Otwinowski, W. Minor, Processing of X-ray diffraction data collected in oscillation mode. *Methods Enzymol.* **276**, 307–326 (1997).
37. L. C. Storoni, A. J. McCoy, R. J. Read, Likelihood-enhanced fast rotation functions. *Acta Crystallogr. D Biol. Crystallogr.* **60**, 432–438 (2004).
38. Collaborative Computational Project, Number 4, The CCP4 suite: Programs for protein crystallography. *Acta Crystallogr. D Biol. Crystallogr.* **50**, 760–763 (1994).
39. G. N. Murshudov, A. A. Vagin, E. J. Dodson, Refinement of macromolecular structures by the maximum-likelihood method. *Acta Crystallogr. D Biol. Crystallogr.* **53**, 240–255 (1997).
40. P. Emsley, B. Lohkamp, W. G. Scott, K. Cowtan, Features and development of Coot. *Acta Crystallogr. D Biol. Crystallogr.* **66**, 486–501 (2010).
41. S. Chaudhury *et al.*, Benchmarking and analysis of protein docking performance in Rosetta v3.2. *PLoS One* **6**, e22477 (2011).
42. S. Lyskov *et al.*, Serverification of molecular modeling applications: The Rosetta online server that includes everyone (ROSIE). *PLoS One* **8**, e63906 (2013).
43. S. Lyskov, J. J. Gray, The RosettaDock server for local protein-protein docking. *Nucleic Acids Res.* **36**, W233–W238 (2008).
44. P. Conway, M. D. Tyka, F. DiMaio, D. E. Konerding, D. Baker, Relaxation of backbone bond geometry improves protein energy landscape modeling. *Protein Sci.* **23**, 47–55 (2014).
45. L. G. Nivón, R. Moretti, D. Baker, A Pareto-optimal refinement method for protein design scaffolds. *PLoS One* **8**, e59004 (2013).
46. H. M. Berman *et al.*, The Protein Data Bank. *Nucleic Acids Res.* **28**, 235–242 (2000).
47. F. Sievers, D. G. Higgins, Clustal Omega for making accurate alignments of many protein sequences. *Protein Sci.* **27**, 135–145 (2018).
48. F. Sievers *et al.*, Fast, scalable generation of high-quality protein multiple sequence alignments using Clustal Omega. *Mol. Syst. Biol.* **7**, 539 (2011).
49. P. J. Cock *et al.*, Biopython: Freely available Python tools for computational molecular biology and bioinformatics. *Bioinformatics* **25**, 1422–1423 (2009).
50. M. Waskom *et al.*, Zenodo (mwaskom/seaborn, Version 0.11.1, 2020). http://doi.org/10.5281/zenodo.4379347. Accessed 15 June 2021.